Neoplasma 2024; 71(6): 571–580

doi:10.4149/neo_2024_240422N179

Disruption of lipid raft reverses drug resistance in colorectal cancer cells through the phosphatase and tensin homolog/phosphoinositide 3-kinase/protein kinase B pathway and P-glycoprotein

Jing CHEN, Wei ZHENG, Qian LI, RanRan XU, TingTing BAI*, Chao PAN*

Zhongshan Hospital Xiamen University, Xiamen, China

**Correspondence: xiao_bai_1210@163.com; panchao@xmu.edu.cn*

Received April 22, 2024 / Accepted December 10, 2024

Regarding flotillin knockdown, drug resistance is reversed in colorectal cancer (CRC) cell lines; this is associated with the phosphoinositide 3-kinase/protein kinase B (PI3K/AKT) pathway, as our previous experimental results indicated. However, the exact mechanism underlying this pathway remains unclear. PI3K inhibitor and activator were added separately to clarify the role of the PI3K pathway in reversing drug resistance. The results showed decreased resistance after inhibiting PI3K activity. Furthermore, the reduced resistance due to flotillin knockdown was restored after adding the PI3K activator. Additional results showed no changes in PI3K molecules. However, p-AKT expression was downregulated. Further results suggested that the phosphatidylinositol (3,4,5)-trisphosphate/phosphatidylinositol 4,5-bisphosphate (PIP3/PIP2) ratio was downregulated, whereas the phosphatase and tensin homolog (PTEN) expression was upregulated. In addition, we also found that P-gp activity inhibition resulted in increased adriamycin accumulation and reversal of resistance, and flotillin knockdown was accompanied by a downregulation of P-gp expression in CRC cells. In conclusion, our study demonstrated that flotillin knockdown could reverse drug resistance in CRC cells by downregulating the PTEN/PI3K/AKT pathway and P-gp.

Key words: colorectal cancer; drug resistance; lipid rafts; PI3K/AKT pathway; P-glycoprotein

Multidrug resistance (MDR) refers to the cross-resistance of cancer cells to several chemotherapeutic agents [1], which is a difficult and urgent concern about chemotherapy. Lipid rafts are small (10–200 nm), heterogeneous, highly dynamic, sterol-and sphingolipid-enriched domains that can separate cellular processes [2]. These contribute to the development of drug resistance regarding multiple malignancies [3–5]. Therefore, disrupting these lipid rafts can restore drug sensitivity in breast cancer-resistant cells [6]. Our preliminary experiments revealed that drug resistance in colorectal cancer (CRC) cells was reversed when the lipid raft-resident proteins, flotillins, were knocked down [7]. However, the exact underlying mechanisms remain unclear. Regarding the phosphoinositide 3-kinase (PI3K) pathway, most of the PI3K/protein kinase B (AKT) positive regulatory molecules such as PI3K, AKT, 3-phosphoinositide-dependent kinase 1 (PDK1), and mammalian target of rapamycin (mTOR) are located in lipid rafts, which facilitate lipid raft-mediated AKT phosphorylation [8, 9], promote phosphatidylinositol (3,4,5)-trisphosphate (PIP3) accumulation at the plasma membrane, and activate downstream signaling molecules [10]. The disruption in the lipid raft inhibits the activation of the PI3K/AKT pathway, such that the pharmacological disruption in its structure inhibits insulin-like growth factor-1-mediated AKT phosphorylation [11]. Moreover, it blocks the binding of AKT and PDK1 to the cell membrane by affecting the PH structural domain, which inhibits the activation of the PI3K/AKT pathway [12]. Therefore, disrupting lipid rafts might inhibit the PI3K/AKT pathway activation. The PI3K signaling pathway is one of the most frequently altered pathways in human cancers and is crucial for driving tumorigenesis and progression [13–19]. PTEN is a tumor suppressor that dephosphorylates PIP3 to PIP2, thereby antagonizing the PI3K pathway [20]. Therefore, activating the PI3K signaling molecules or inactivating the PTEN molecules is manifested as the aberrant activation of the PI3K/AKT signaling pathway, which promotes cell growth, proliferation, metabolism, migration, and secretion.

This aberrant activation is closely associated with tumorigenesis, proliferation, apoptosis, invasion, metastasis, epithelial-mesenchymal transition, the immune microenvironment, and drug resistance [21–28].

Materials and methods

Cell culture. The human colon cancer cell line (HCT-15) (China Center for Type Culture Collection and Cell Bank of the Chinese Academy of Sciences, Shanghai, China; Serial: TCHu133) was cultured in a medium (RPMI-1640, Gibco, USA; #A4192301) supplemented with 1% penicillin-streptomycin (Gibco, #15140122) and 10% fetal bovine serum (FBS, Hyclone, USA, #SH30071.03E) at 37 °C with 5% carbon dioxide (CO_2). HCT-15 cells were placed in adriamycin (ADM, Med Chem Express, USA; #HY-15142) solution at a concentration of 10 μg/ml for 2 h and repeated several times until the cell death rate of tumor cells in a medium with ADM concentration of 0.4–0.5 μg/ml was <5% (Supplementary Figure S1).

Lentiviral transduction. Well-grown HCT-15/ADM cells were inoculated into 6-well plates and cultured for 24 h. The cells were then infected with a lentivirus pre-packaged in our laboratory. Flotillin-1 (NM_005803. 3) and Flotillin-2 (NM_004475.2) were retrieved from the National Center for Biotechnology Information (NCBI) website. The short hairpin RNA refers to the previous literature [7]. Puromycin was added 72 h later to a final concentration of 2 μg/ml; the cells were cultured continuously for 4–5 days to screen for stabilized strains.

Lipid raft labeling and confocal microscopy imaging. A coverslip was placed in a 6-well plate so that the cells could adhere to the glass coverslip for growth; the cells were incubated for 24 h. Phosphate-buffered saline (PBS, Beijing Solarbio Science, China; #P1020) was used to wash the cells three times. Live cells were incubated with cholera toxin subunit B (recombinant), Alexa Fluor™ 555 conjugate (#C34776) (CT-B AF555, Vybrant Lipid Raft Labeling Kits, Thermo, USA) at a concentration of 1 μg/ml. The plate was incubated for 20 min at 4 °C, protected from light. PBS was used to re-wash the cells three times. After incubation with paraformaldehyde (4%) for 15 min at approximately 28 °C the cells were re-washed thrice with PBS, and Hoechst33258 (Beyotime Biotechnology, China; #C1017) was used for nuclear staining while avoiding light for 15 min at room temperature. Finally, the cells were observed under confocal fluorescence microscopy (Olympus, Japan; 400× lens).

Cell Counting Kit-8. Cell viability was assessed using the Cell Counting Kit-8 (CCK-8) assay (Bimake, USA; #B34302) following the manufacturer's instructions. The cells were placed into 96-well plates with 3×10^3 cells/well. The cells were incubated at 37 °C with 5% CO_2 for 24 h. Furthermore, a gradient concentration of ADM from 0 to 64 μg/ml was added to the culture medium and incubated for 24 h. In addition, 110 μM of CCK-8 reagent and medium mixture were added to each well; the ratio of CCK-8 reagent to the medium was 10:100, and the mixture was incubated for 2 h. The optical density of 450 nm value was measured, and the proliferation inhibition rate of each group of cells was calculated.

ADM accumulation. Cells were spread in 6-well plates with 5×10^5 cells/well and 3 replicate wells. The cells were incubated at 37 °C with 5% CO_2 for 24 h. ADM concentration of 20 μg/ml was added; 0.1% DMSO (MP biomedicals, USA) was added to the control group. After the incubation for 2.5 h, the cells were washed three times with PBS buffer, trypsin-digested, collected, and centrifuged at 1,000×g/4 °C for 5 min. The supernatant was discarded and washes were repeated 3 times with PBS buffer. Finally, the cells were resuspended with 1 ml of PBS buffer (pre-cooled at 4 °C). ADM fluorescence intensity was detected by flow cytometry (excitation wavelength: 488 nm, emission wavelength: 575 nm).

Enzyme-linked immunosorbent assay. PIP3 (#JL19768) and PIP2 (#JL13826) levels were assayed using an enzyme-linked immunosorbent assay kit (Jianglai Biotechnology Co. Ltd. Shanghai, China) manual. The cells were washed with PBS 3 times, trypsin digestion was performed to collect the cells that were resuspended with 1ml of PBS. The cells were then broken by ultrasonic waves and centrifuged at 4 °C; 3,000×g for 20 min; the supernatant was collected. Sequentially horseradish peroxidase (HRP)-labeled antibody (100 μl), substrate A (50 μl), and substrate B (50 μl), were incubated at 37 °C for 15 min away from light. The optical density of each well was then measured at 450 nm.

Western blot. The cells were lysed with a mixture of radioimmunoprecipitation assay buffer (Beyotime, China; #P0013B), Protease Inhibitor (Applygen, China; #P1265-1), and Phosphatase Inhibitor (Applygen; #P1260-1) (100:1:1) and quantified using the bicinchoninic acid (Beijing Solarbio Science; #PC0020) assay. The protein lysate was mixed with loading buffer and boiled at 100 °C for 10 min. Equal amounts of protein lysates were separated by electrophoresis on a 10% sodium dodecyl sulfate-polyacrylamide gel and transferred into a polyvinylidene difluoride membrane. The membrane was immersed in Tween-20 (Beyotime Biotechnology, China; #ST828) triple buffered saline (TBST) containing 5% skimmed milk powder for 2 h at room temperature; then the primary (overnight incubation) and secondary antibodies (2 h) were added. The protein bands were detected by a chemiluminescent horseradish peroxidase substrate. The assayed proteins included PI3K p110 α (#4249s), PI3K p110 β (#3011s), AKT (pan) (#4691s), Phospho-AKT(Ser473) (#4060s), PTEN (#9559s) (Cell Signaling Technology, USA; dilution ratio 1:1000), anti-flotillin 1 (#15571-1-AP), anti-flotillin 2 (#28208-1-AP), P-gp antibodies (#22336-1-AP) (Proteintech Group, China; dilution ratio 1:1000), GAPDH monoclonal antibody (#60004-1-Ig) (Proteintech Group, China, dilution ratio 1:10000), and Phospho-PI3K p85

(Tyr458) [Tyr467]/p55 (Tyr199) (#AF3242) (Affinity Biosciences, USA; dilution ratio 1:1000).

Statistical analyses. The data obtained in this experiment are expressed as mean ± standard deviation (S) and were statistically analyzed using GraphPad Prism version 8.0 (San Diego, USA). Statistical results were tested for significance using a t-test or one-way analysis of variance. Statistical significance was set at $p<0.05$.

Results

Knockdown of flotillin-1 and flotillin-2 inhibits lipid raft formation and reverses drug resistance in HCT-15-resistant cell lines with CRC. Empty vector, knockdown flotillin-1, and knockdown flotillin-2 cell lines were denoted as Con, Flot1-RNAi, and Flot2-RNAi, respectively. First, we used cholera toxin subunit B (recombinant), Alexa Fluor™ 555 conjugate (CT-B AF555), a lipid raft staining marker, to detect the expression of lipid rafts after flotillin knockdown; the results showed that the expression of lipid rafts was downregulated after flotillin knockdown (Figure 1A). Flotillin-1 and flotillin-2 knockdown resulted in increased sensitivity of resistant cells to ADM (Figures 1B, 1C), and resistance reversal.

The PI3K/AKT pathway is involved in regulating drug resistance in CRC cells. Therefore, to verify whether the PI3K pathway could regulate the drug resistance in CRC cells, we inhibited and activated the PI3K pathway and observed each group's changes in drug resistance. However, to ensure that the inhibition and activation were effective, we measured

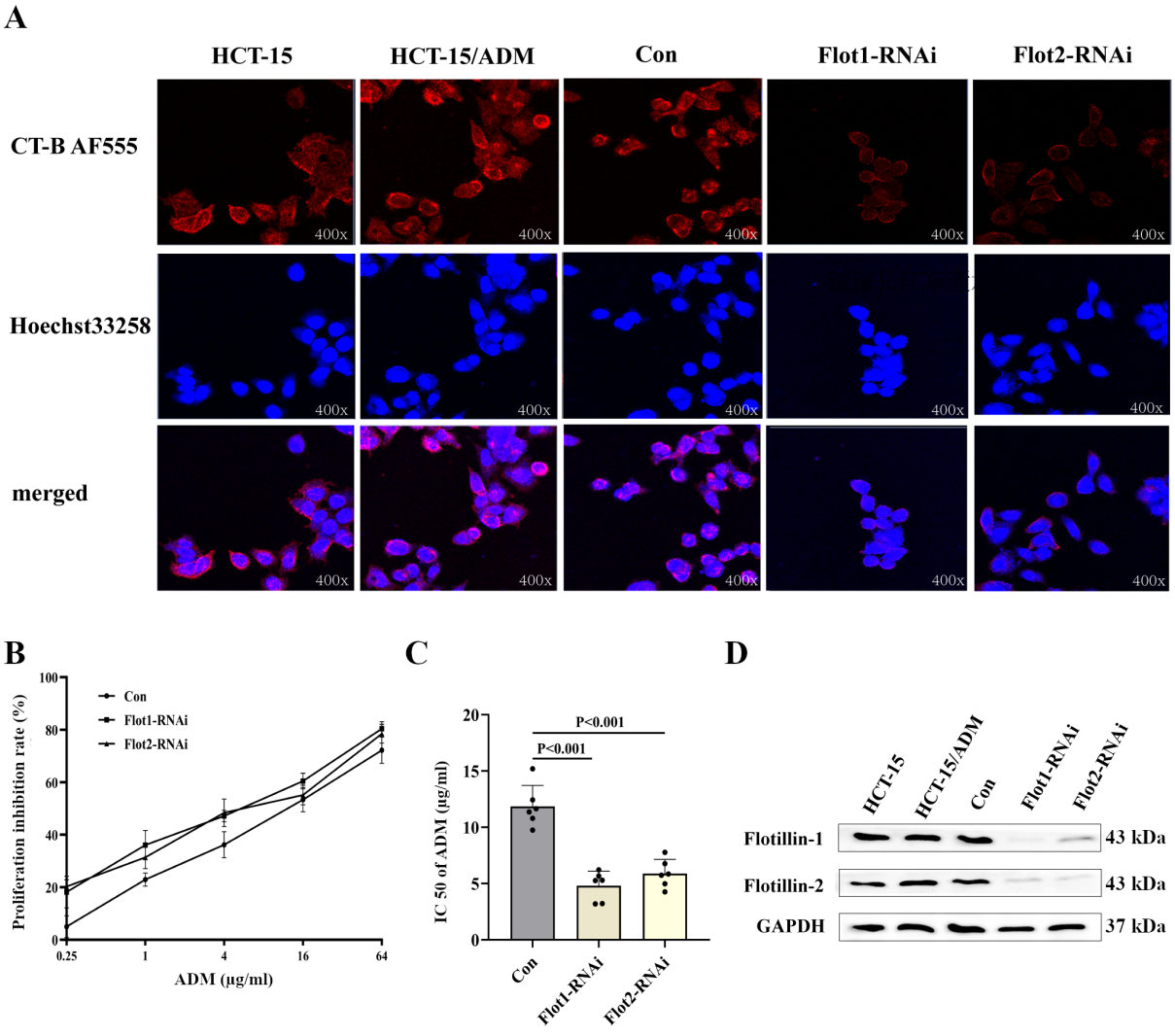

Figure 1. Effect of flotillin-1 or flotillin-2 knockdown on lipid rafts, proliferation, and ADM resistance in HCT-15/ADM cells. A) CT -B AF555 staining was used to label lipid rafts, and nuclear staining (Hoechst 33258) and confocal microscopy analysis (magnification: 400×) were performed. B) Flotillin-1 and flotillin-2 knockdown HCT-15/ADM cells show increased sensitivity to the effects of ADM treatment. C) IC50 ADM values are decreased in flotillin-1 and flotillin-2 knockdown HCT-15/ADM cells. D) Flotillin-1 and flotillin-2 expressions significantly decrease after the flotillin-1 knockdown, and the flotillin-1 and flotillin-2 expressions are markedly depressed after the flotillin-2 knockdown.

the PIP3/PIP2 values to represent the PI3K pathway activity. First, we tested the appropriate time and concentration of the PI3K activator (740Y-P) in group flotillin-1 RNAi. The results showed that 50 μM 740-YP increased the survival of HCT-15/ADM cells cultivated in gradually increasing concentrations of ADM (0.25, 1, 4, 16, and 64 μg/ml) (Figure 2A). Furthermore, we tested for the appropriate concentration of the PI3K inhibitor (GDC-0941) (the selected time was 24 h) to ensure the comparability of the results of the subsequent experiments. The results showed that the concentration was 0.5–8 μM; the cell viability significantly decreased with increasing concentration. However, at 8 μM, there was excessive cell death. Therefore, we selected a concentration of 4 μM (Figure 2B). After adding 740Y-P, PIP3/PIP2 values were upregulated in the HCT-15, Con, flotillin-1-RNAi, and flotillin-2-RNAi groups, with the most significant upregulation occurring in the flotillin-2-RNAi group. However, there was no significant change in the HCT-15/ADM group (Figure 2C, Supplementary Table S1). Conversely, drug resistance was upregulated in the flotillin-1-RNAi and flotillin-

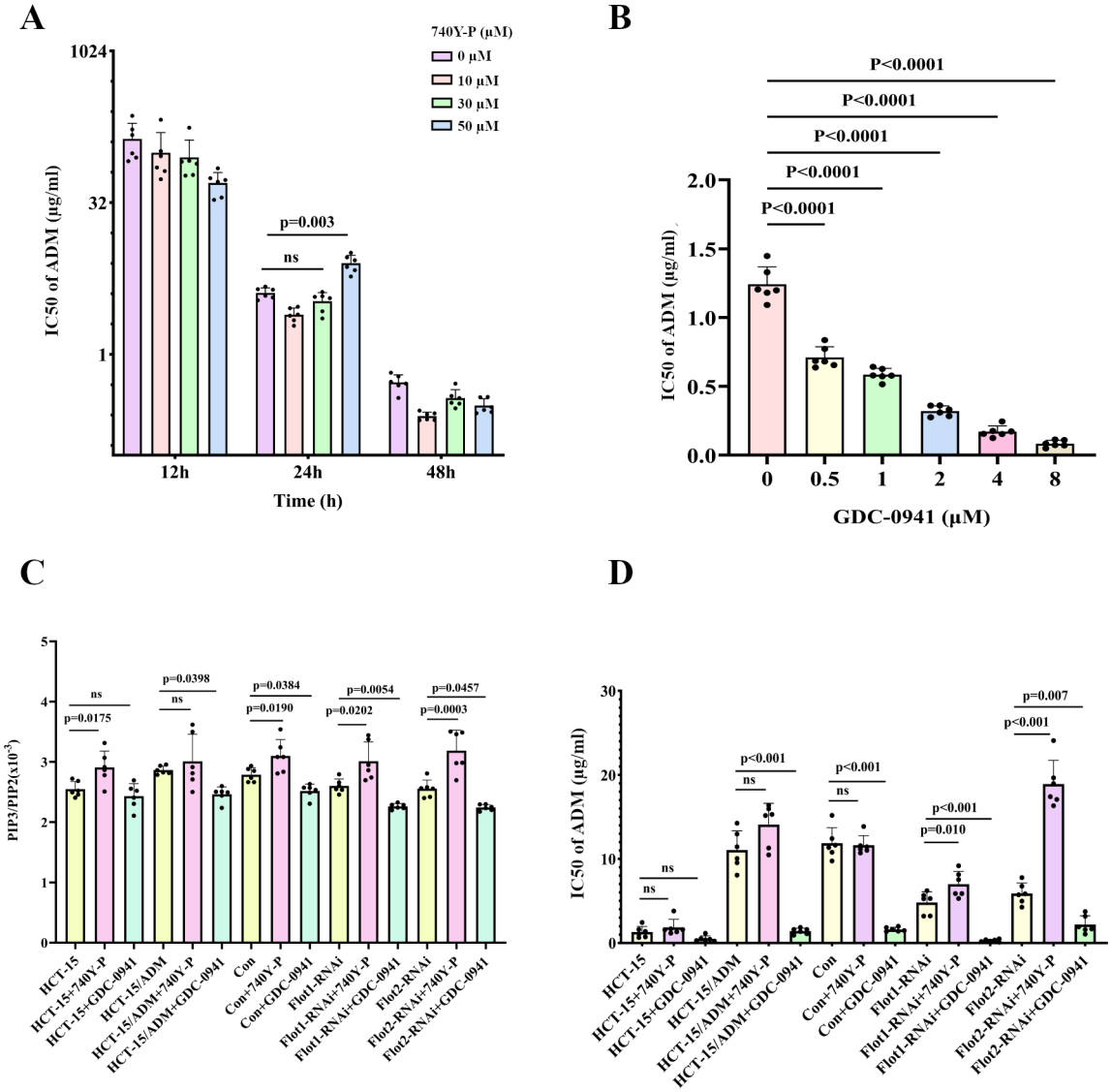

Figure 2. Effects of adding PI3K activator and inhibitor on PI3K pathway activity, resistance to ADM in various tumor cells. A) IC50 values of flotillin-1-RNAi in the ADM concentration of 0, 0.25, 1, 4, 16, 64 μg/ml, respectively, after 740Y-P is added at 12 h, 24 h, and 48 h and concentrations of 0, 10, 30, and 50 μM, respectively. B) IC50 values of flotillin-1-RNAi in the ADM concentration of 0, 0.25, 1, 4, 16, 64 μg/ml, respectively, after GDC-0941 is added at concentrations of 0, 0.5, 1, 2, 4, and 8 μM, respectively, for 24 h. C) ELISA is used to detect the values of PIP3 and PIP2 after adding the PI3K activator for 24 h (740Y-P, at a concentration of 50 μM) and inhibitor (GDC-0941, at a concentration of 4 μM) in each group, and their ratios are compared. D) CCK-8 assay in the ADM concentration of 0.25, 1, 4, 16, 64 μg/ml, respectively, with or without the addition of 740Y-P (concentration of 50 μM), with or without adding GDC-0941 (concentration of 4 μM), the role of 24 h, and the absorbance of the cells in each group is used to obtain the changes in the IC50 of the tumor cells in each group after calculating the inhibition rate of proliferation.

2-RNAi groups (Figure 2D). Moreover, the drug resistance of the flotillin-2-RNAi group was significantly ($p<0.001$) upregulated or even exceeded that of the corresponding Con group after adding the activator. The remaining three groups, HCT-15, HCT-15/ADM, and Con, showed no significant changes (Figure 2D, Supplementary Table S2). After adding GDC-0941, PIP3/PIP2 values decreased in all groups except for the HCT-15 group, whereas there was no significant difference between the flotillin-1 and flotillin-2 knockdown (Figure 2C, Supplementary Table S3). Simultaneously, drug resistance was downregulated in all resistant cell lines, with or without flotillin protein knockdown, except for the HCT-15 group. Among them, the HCT-15/ADM and Con groups showed downregulation to a similar extent; the flotillin-1 cell line knockdown was significantly ($p<0.001$) downregulated after adding the PI3K inhibitor. It was less resistant than the HCT-15 group without ADM induction. The knockdown flotillin-2 cell line was partially downregulated and to a lesser extent than the knockdown flotillin-1 cell line (Figure 2D, Supplementary Table S4).

Flotillin knockdown reverses drug resistance in CRC cells through the PTEN/PI3K/AKT pathway. These results showed that inhibition of PI3K activity reversed tumor cell resistance, whereas activation of PI3K activity in knockdown flotillin cells increased tumor cells' resistance to ADM (Figure 2D), which demonstrated that the PI3K pathway regulated drug resistance in CRC cells. Furthermore, we identified the specific molecules involved in the PI3K pathway and examined critical molecules in various parts of the PI3K pathway. First, p-AKT expression was downregulated after flotillin knockdown (Figures 3A, 3B). Notably, the PI3K expression was not changed. In knockdown flotillin cells, we confirmed the downregulation of PI3K pathway activity by detecting the PIP3/PIP2 value, which was downregulated (Figure 2C). Therefore, we detected the expression of PTEN, a critical antagonist of the PI3K pathway, and found that it was upregulated (Figures 3A, 3B). Additionally, PTEN expression was not significantly downregulated in the flotillin-1-RNAi group after adding PI3K inhibitor, whereas it was significantly downregulated in the flotillin-2-RNAi group (Figure 3A). Expressions in the flotillin-1-RNAi and flotillin-2-RNAi groups were significantly upregulated after adding the PI3K activator, whereas P-AKT was significantly upregulated in the flotillin-2-RNAi group and to a lesser extent in the flotillin-1-RNAi group (Figure 3B).

Flotillin knockdown reverses drug resistance in CRC cells by downregulating P-gp expression. One of the characteristics of MDR cells is increased drug efflux, a substrate for the drug-resistant protein ABCB1 (P-gp). Therefore, we investigated the accumulation of ADM in parental and MDR cells and changes after flotillin knockdown. The results showed that ADM accumulation in drug-resistant cells was significantly smaller than that in parental cells after 2.5 h of incubation with ADM, suggesting that drug efflux was more pronounced in drug-resistant cells. In contrast, in the flotillin knockdown group, ADM accumulation increased than that in the Con group, indicating that ADM efflux was reduced in knockdown flotillins. ADM accumulation was significantly increased in all tumor cell groups after P-gp activity was inhibited (Figure 4A, Supplementary Table S5). However, the change in ADM accumulation indicated a change in drug efflux, which might be associated with P-gp expression. Therefore, we examined the P-gp expression after flotillin knockdown. Furthermore, the downregulation of P-gp expression was observed after flotillin knockdown (Figure 4B). In addition, flotillin knockdown reversed drug resistance in CRC cells, which was significantly reduced in all tumor cell groups after the inhibition of P-gp activity (Figure 4C, Supplementary Table S6). The above results revealed that P-gp was crucial for regulating drug resistance

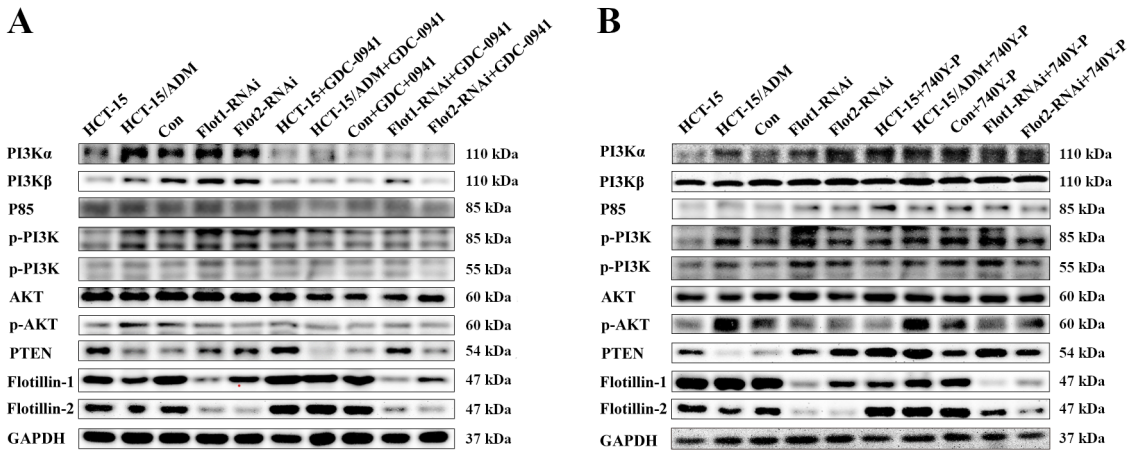

Figure 3. Effects of adding PI3K activator and inhibitor on protein expression of key molecules of the PI3K pathway. A) The expression of key molecules of the PI3K pathway in each group and changes after adding the PI3K inhibitor (GDC-0941, at a concentration of 4 μM). B) The expression of key molecules of the PI3K pathway in each group and changes after adding the PI3K activator (740Y-P, at a concentration of 50 μM).

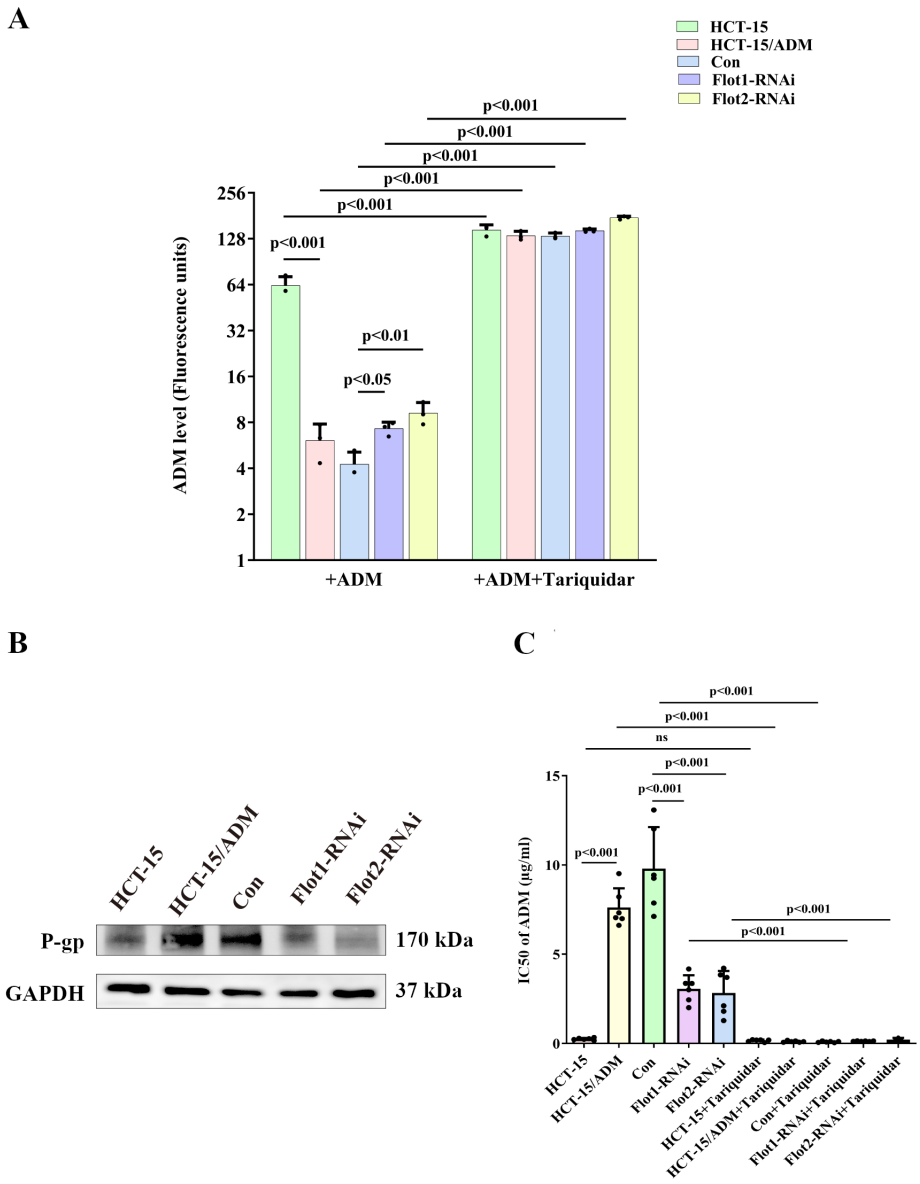

Figure 4. Expression of P-gp protein and changes in ADM accumulation and resistance to ADM after inhibition of P-gp activity in various tumor cells. A) ADM accumulation changes after the addition of the P-gp inhibitor (Tariquidar, concentration of 1 μM), ADM (concentration of 20 μg/ml), for 2.5 h. ADM accumulation increased after flotillin knockdown and decreased significantly after P-gp inhibition. B) Expression of P-gp. C) IC50 values of tumor cells in the ADM concentration of 0, 0.25, 1, 4, 16, and 64 μg/ml, respectively, after the inhibition of P-gp activity (Tariquidar, concentration of 1 μM, time 24 h).

in CRC cells. Furthermore, flotillin knockdown could reverse drug resistance in intestinal cancer cells by downregulating the expression of P-gp.

Discussion

Based on our preliminary experiments, we investigated the mechanisms through which disruption in lipid rafts could reverse drug resistance in CRC cells, which might be associated with the PI3K pathway [7]. In this study, drug resistance was downregulated in all groups (with or without resistance, flotillin knockdown) in the presence of GDC-0941. GDC-0941 (pictilisib) is a selective class I PI3K inhibitor that potently inhibits all four isoforms of class I PI3K and the activity of the PI3K/AKT pathway without inhibiting other molecular targets. The PI3K pathway is involved in forming and reversing drug resistance in several malignant tumors [29–32]. However, whether the pathway could be involved in flotillin knockdown to disrupt the structure of lipid rafts remains unclear, thereby reversing drug resistance in CRC

cells. Notably, to investigate this further, a PI3K activator (740Y-P is an EGFR analog that activates the PI3K/AKT pathway through the cell membrane) was used inside the experimental group; if flotillin knockdown reverses resistance by inhibiting PI3K pathway activity, the resistance will then be restored in the flotillin knockdown experimental group. As expected, flotillin-1 knockdown and the activation of PI3K activity partially restored resistance. Flotillin-2 knockdown completely restored resistance, whereas the other groups without flotillin knockdown showed no significant change in resistance. In addition, the results showed that flotillin-1 knockdown was inconsistent with the degree of recovery from drug resistance after adding PI3K activator to flotillin-2 knockdown. Therefore, the critical role of the PI3K pathway in this process was confirmed; the specific molecular targets of the PI3K pathway were further explored. Two crucial catalytic PI3K subunits, p110α and p110β (p110γ and p110δ are mainly present in lymphocytes and could not be detected in these present experiments). In addition, the regulatory subunit (p85) and active forms of PI3K (p-PI3K) and p-AKT were detected. We found that p-AKT expression was downregulated; however, notably, the PI3K-related molecules were not changed; this contradicts our previous experimental results [7], which showed a downregulation of the expression of PI3K p110β when the flotillins were knocked down. This could be associated with the different experimental conditions in our previous experiments, where low ADM concentrations were still used to maintain resistance. However, in this experiment, to better reflect clinical reality, ADM was no longer added after flotillin knockdown. Furthermore, the value of PIP3/PIP2 was examined, which could be used as a more sensitive indicator of PI3K activity [33]; the ratio was downregulated after flotillin knockdown. The PI3K pathway is positively and negatively regulated [17, 34]. Therefore, we assessed PTEN expression and found that flotillin knockdown downregulated PTEN expression. This explains why there was no change in PI3K-related molecules after flotillin knockdown, whereas the PI3K/AKT pathway activity was downregulated. Therefore, we propose that tumor cells reverse drug resistance in CRC cases after flotillin knockdown by upregulating PTEN expression, downregulating PIP3/PIP2, and further inhibiting the PI3K/AKT pathway activity. Notably, the activation of PI3K after flotillin-2 knockdown resulted in a complete recovery of drug resistance, which was significantly higher than that after activating PI3K in the null group. However, activating PI3K after flotillin-2 knockdown resulted in a higher value of PIP3/PIP2 than that of the corresponding null group, which was not observed with flotillin-1 knockdown. This indicated that PI3K was better activated after flotillin-2 knockdown. This could be because, in our experiments, we observed that the PI3K pathway was reactivated after flotillin-1 and flotillin-2 knockdown, and the upregulation of PTEN in the flotillin-2 knockdown group was smaller than that in the flotillin-1 knockdown group: the antagonism to the activation of the PI3K/AKT pathway was weaker. Furthermore, the interaction between flotillin-1 and flotillin-2 in this experiment showed that flotillin-1 expression was downregulated after flotillin-2 knockdown, whereas flotillin-2 was downregulated more significantly after flotillin-1 knockdown. Similarly, the experimental results after flotillin-1 and flotillin-2 knockdowns were inconsistent. p-AKT and p-extracellular signal-regulated kinase 1 (pERK) expression was downregulated after flotillin-2 knockdown in the breast cancer MCF7 cell line. However, p-AKT and p-ERK did not change significantly after flotillin-1 knockdown. Similar results were observed in the breast cancer SKBR3 cells [35]. It has been suggested that this discrepancy is because flotillin-2 can directly or indirectly affect flotillin-1, as flotillin-1 was destabilized after flotillin-2 knockdown in experiments [36]. This is not entirely consistent with our experimental results, suggesting that the interactions between flotillins may be mutual. This interaction resulted in different results for flotillin-1 and flotillin-2 under the same experimental conditions; this interaction requires further investigation. In addition, flotillin-1 knockdown followed by the use of PI3K inhibitor PI3K inhibitor resulted in the downregulation of tumor cell resistance to a level similar to that in the parental cell line after using PI3K inhibitor, suggesting that flotillin-1 knockdown combined with using PI3K inhibitor resulted in the complete reversal of drug resistance. Further in-depth studies might be a high-quality solution for reversing tumor cell resistance in clinical practice.

The presence of P-gp, a transmembrane protein, outside the lipid raft region has been reported. However, more studies have suggested that P-gp is present within the lipid rafts [37]. Changes in membrane structure-lipid rafts have been found to modulate P-gp activity: inducing P-gp out of the lipid raft region inhibits its activity [38]. Moreover, disruption in the lipid raft structure by methyl-β-cyclodextrin leads to P-gp displacement and loss of function [39]. This may be due to changes in the membrane microenvironment [40]. However, the use of methyl-β-cyclodextrin disrupts the structure of lipid rafts and simultaneously disrupts the fluidity and permeability of cell membranes. Previously, no effect of flotillin knockdown on P-gp has been reported in the literature. However, in our study, drug resistance was downregulated in all resistant tumor cells (with or without flotillin knockdown) after the P-gp inhibitor was applied. Furthermore, we found that flotillin knockdown resulted in the downregulation of P-gp expression. Simultaneously, an increase in ADM accumulation was observed, indicating a decrease in drug efflux, which we hypothesized to be associated with a reduction in P-gp activity. Conversely, it has been shown that PI3K/AKT can regulate P-gp expression; the exact mechanism of this regulation is not known [41, 42]. Therefore, further research is needed to explore the specific mechanisms of P-gp changes.

This study has some limitations. First, these results were only validated in the HCT-15 cell line; whether the same

results can be found in other cell lines with CRC needs further verification. Second, we did not obtain data using clinical patient specimens; therefore, additional studies are required. Furthermore, we found that after flotillin knockdown, P-gp expression was downregulated, and drug resistance was reversed simultaneously. At present, whether the P-gp change could be due to changes in lipid raft structure or the inhibition of the PI3K pathway is unclear; further clarification is needed. Furthermore, the mechanism underlying the PTEN regulation of PIP3 could not be directly demonstrated. Other modes of PIP3 regulation, such as inositol polyphosphate 5 phosphatase, convert PIP3 to PIP2 [43]. In addition, revealing the mechanism through which flotillins regulate PTEN was not possible, with some studies suggesting that PTEN is localized in the non-lipid raft region and separated from signaling molecules such as PI3K and AKT, which are localized in lipid rafts [10, 44]. Therefore, disrupting the lipid raft structure may lead to PTEN translocation and thus antagonize the PI3K/AKT pathway. However, the direct interaction mechanism between flotillins and PTEN remains clear and will be further explored in subsequent experiments. In addition, studies to observe the effect of drug resistance reversal after flotillin knockdown in PTEN expression-deficient tumors and drug resistance reversal flotillin knockdown in vivo are lacking and need to be conducted.

Supplementary information is available in the online version of the paper.

Acknowledgments: This study was sponsored by the Fujian Provincial Health Technology Project (Project No.: 2023QNB006) and the Medical Innovation Project of the Fujian Province 2021CXB022. The authors would like to thank for the support of Zhongshan Hospital Xiamen University, Xiamen, China.

References

[1] WU CP, HSIAO SH, WU YS. Perspectives on drug repurposing to overcome cancer multidrug resistance mediated by ABCB1 and ABCG2. Drug Resist Updat 2023; 71: 101011. https://doi.org/10.1016/j.drup.2023.101011

[2] SEZGIN E, LEVENTAL I, MAYOR S, EGGELING C. The mystery of membrane organization: composition, regulation and roles of lipid rafts. Nat Rev Mol Cell Biol 2017; 18: 361–374. https://doi.org/10.1038/nrm.2017.16

[3] LEE WK, KOLESNICK RN. Sphingolipid abnormalities in cancer multidrug resistance: Chicken or egg? Cell Signal 2017; 38: 134–145. https://doi.org/10.1016/j.cellsig.2017.06.017

[4] BONACINA F, PIRILLO A, CATAPANO AL, NORATA GD. Cholesterol membrane content has a ubiquitous evolutionary function in immune cell activation: the role of HDL. Curr Opin Lipidol 2019; 30: 462–469. https://doi.org/10.1097/mol.0000000000000642

[5] GU L, SAHA ST, THOMAS J, KAUR M. Targeting cellular cholesterol for anticancer therapy. FEBS J 2019; 286: 4192–4208. https://doi.org/10.1111/febs.15018

[6] RAGHAVAN V, VIJAYARAGHAVALU S, PEETLA C, YAMADA M, MORISADA M et al. Sustained Epigenetic Drug Delivery Depletes Cholesterol-Sphingomyelin Rafts from Resistant Breast Cancer Cells, Influencing Biophysical Characteristics of Membrane Lipids. Langmuir 2015; 31: 11564–11573. https://doi.org/10.1021/acs.langmuir.5b02601

[7] YE DM, YE SC, YU SQ, SHU FF, XU SS et al. Drug-resistance reversal in colorectal cancer cells by destruction of flotillins, the key lipid rafts proteins. Neoplasma 2019; 66: 576–583. https://doi.org/10.4149/neo_2018_180820N633

[8] MOLLINEDO F, GAJATE C. Lipid rafts as major platforms for signaling regulation in cancer. Adv Biol Regul 2015; 57: 130–146. https://doi.org/10.1016/j.jbior.2014.10.003

[9] REIS-SOBREIRO M, ROUE G, MOROS A, GAJATE C, DE LA IGLESIA-VICENTE J et al. Lipid raft-mediated Akt signaling as a therapeutic target in mantle cell lymphoma. Blood Cancer J 2013; 3: e118. https://doi.org/10.1038/bcj.2013.15

[10] GAO X, LOWRY PR, ZHOU X, DEPRY C, WEI Z et al. PI3K/Akt signaling requires spatial compartmentalization in plasma membrane microdomains. Proc Natl Acad Sci U S A 2011; 108: 14509–14514. https://doi.org/10.1073/pnas.1019386108

[11] ROMANELLI RJ, MAHAJAN KR, FULMER CG, WOOD TL. Insulin-Like Growth Factor-I-Stimulated Akt Phosphorylation and Oligodendrocyte Progenitor Cell Survival Require Cholesterol-Enriched Membranes. J Neurosci Res 2009; 87: 3369–3377. https://doi.org/10.1002/jnr.22099

[12] CALAY D, VIND-KEZUNOVIC D, FRANKART A, LAMBERT S, POUMAY Y et al. Inhibition of Akt Signaling by Exclusion from Lipid Rafts in Normal and Transformed Epidermal Keratinocytes. J Invest Dermatol 2010; 130: 1136–1145. https://doi.org/10.1038/jid.2009.415

[13] LIEN EC, DIBBLE CC, TOKER A. PI3K signaling in cancer: beyond AKT. Curr Opin Cell Biol 2017; 45: 62–71. https://doi.org/10.1016/j.ceb.2017.02.007

[14] FRUMAN DA, CHIU H, HOPKINS BD, BAGRODIA S, CANTLEY LC et al. The PI3K Pathway in Human Disease. Cell 2017; 170: 605–635. https://doi.org/10.1016/j.cell.2017.07.029

[15] JANKU F, YAP TA, MERIC-BERNSTAM F. Targeting the PI3K pathway in cancer: are we making headway? Nat Rev Clin Oncol 2018; 15: 273–291. https://doi.org/10.1038/nrclinonc.2018.28

[16] FRUMAN DA, ROMMEL C. PI3K and cancer: lessons, challenges and opportunities. Nat Rev Drug Discov 2014; 13: 140–156. https://doi.org/10.1038/nrd4204

[17] YANG J, NIE J, MA X, WEI Y, PENG Y et al. Targeting PI3K in cancer: mechanisms and advances in clinical trials. Mol Cancer 2019; 18: 26. https://doi.org/10.1186/s12943-019-0954-x

[18] VANHAESEBROECK B, LEEVERS SJ, PANAYOTOU G, WATERFIELD MD. Phosphoinositide 3-kinases: A conserved family of signal transducers. Trends Biochem Sci 1997; 22: 267–272. https://doi.org/10.1016/s0968-0004(97)01061-x

[19] HUANG CH, MANDELKER D, SCHMIDT-KITTLER O, SAMUELS Y, VELCULESCU VE et al. The structure of a human p110α/p85α complex elucidates the effects of oncogenic PI3Kα mutations. Science 2007; 318: 1744–1748. https://doi.org/10.1126/science.1150799

[20] JIANG N, DAI Q, SU X, FU J, FENG X et al. Role of PI3K/AKT pathway in cancer: the framework of malignant behavior. Mol Biol Rep 2020; 47: 4587–4629. https://doi.org/10.1007/s11033-020-05435-1

[21] LEIPHRAKPAM PD, ARE C. PI3K/Akt/mTOR Signaling Pathway as a Target for Colorectal Cancer Treatment. Int J Mol Sci 2024; 25: 3178. https://doi.org/10.3390/ijms25063178

[22] ZHANG J, HU Y, ZHOU Y, LIU J, ZHANG S. Effects of PI3K inhibitor NVP-BKM120 on overcoming drug resistance and eliminating cancer stem cell in human breast cancer cells. J Clin Oncol 2015; 33. https://doi.org/10.1200/jco.2015.33.15_suppl.e13509

[22] LIU B, WANG C, CHEN P, CHENG B, CHENG Y. RACK1 induces chemotherapy resistance in esophageal carcinoma by upregulating the PI3K/AKT pathway and Bcl-2 expression. Onco Targets Ther 2018; 11: 211–220. https://doi.org/10.2147/ott.S152818

[24] YANG X, DING Y, XIAO M, LIU X, RUAN J et al. Antitumor compound RY10-4 suppresses multidrug resistance in MCF-7/ADR cells by inhibiting PI3K/Akt/NF-κB signaling. Chem Biol Interact 2017; 278: 22–31. https://doi.org/10.1016/j.cbi.2017.10.008

[25] NI Z, YI J. Oxymatrine induces nasopharyngeal cancer cell death through inhibition of PI3K/AKT and NF-κB pathways. Mol Med Rep 2017; 16: 9701–9706. https://doi.org/10.3892/mmr.2017.7822

[26] ZHANG L, LI Y, WANG Q, CHEN Z, LI X et al. The PI3K subunits, P110α and P110β are potential targets for overcoming P-gp and BCRP-mediated MDR in cancer. Mol Cancer 2020; 19: 10. https://doi.org/10.1186/s12943-019-1112-1

[27] WU H, WANG K, LIU W, HAO Q. PTEN overexpression improves cisplatin-resistance of human ovarian cancer cells through upregulating KRT10 expression. Biochem Biophys Res Commun 2014; 444: 141–146. https://doi.org/10.1016/j.bbrc.2014.01.014

[28] WU H, CAO Y, WENG D, XING H, SONG X et al. Effect of tumor suppressor gene PTEN on the resistance to cisplatin in human ovarian cancer cell lines and related mechanisms. Cancer Lett 2008; 271: 260–271. https://doi.org/10.1016/j.canlet.2008.06.012

[29] JIANG W, ZHONG S, CHEN Z, QIAN J, HUANG X et al. 2D-CuPd nanozyme overcome tamoxifen resistance in breast cancer by regulating the PI3K/AKT/mTOR pathway. Biomaterials 2023; 294: 121986. https://doi.org/10.1016/j.biomaterials.2022.121986

[30] HASHEMI M, TAHERIAZAM A, DANEII P, HASSANPOUR A, KAKAVAND A et al. Targeting PI3K/Akt signaling in prostate cancer therapy. J Cell Commun Signal 2023; 17: 423–443. https://doi.org/10.1007/s12079-022-00702-1

[31] PASKEH MDA, GHADYANI F, HASHEMI M, ABBASPOUR A, ZABOLIAN A et al. Biological impact and therapeutic perspective of targeting PI3K/Akt signaling in hepatocellular carcinoma: Promises and Challenges. Pharmacol Res 2023; 187: 106553. https://doi.org/10.1016/j.phrs.2022.106553

[32] WEI L, MA X, HOU Y, ZHAO T, SUN R et al. Verteporfin reverses progestin resistance through YAP/TAZ-PI3K-Akt pathway in endometrial carcinoma. Cell Death Dis 2023; 9: 30. https://doi.org/10.1038/s41420-023-01319-y

[33] COSTA C, EBI H, MARTINI M, BEAUSOLEIL SA, FABER AC et al. Measurement of PIP3 Levels Reveals an Unexpected Role for p110β in Early Adaptive Responses to p110α-Specific Inhibitors in Luminal Breast Cancer. Cancer Cell 2015; 27: 97–108. https://doi.org/10.1016/j.ccell.2014.11.007

[34] YU L, WEI J, LIU P. Attacking the PI3K/Akt/mTOR signaling pathway for targeted therapeutic treatment in human cancer. Sem Cancer Biol 2022; 85: 69–94. https://doi.org/10.1016/j.semcancer.2021.06.019

[35] ASP N, PUST S, SANDVIG K. Flotillin depletion affects ErbB protein levels in different human breast cancer cells. Biochim Biophys Acta 2014; 1843: 1987–1996. https://doi.org/10.1016/j.bbamcr.2014.04.013

[36] SOLIS GP, HOEGG M, MUNDERLOH C, SCHROCK Y, MALAGA-TRILLO E et al. Reggie/flotillin proteins are organized into stable tetramers in membrane microdomains. Biochem J 2007; 403: 313–322. https://doi.org/10.1042/bj20061686

[37] ORLOWSKI S, MARTIN S, ESCARGUEIL A. P-glycoprotein and 'lipid rafts': some ambiguous mutual relationships (floating on them, building them or meeting them by chance?). Cell Mol Life Sci 2006; 63: 1038–1059. https://doi.org/10.1007/s00018-005-5554-9

[38] GHETIE MA, CRANK M, KUFERT S, POP I, VITETTA E. Rituximab but not other anti-CD20 antibodies reverses multidrug resistance in 2 B lymphoma cell lines, blocks the activity of P-glycoprotein (P-gp), and induces P-gp to translocate out of lipid rafts. J Immunother 2006; 29: 536–544. https://doi.org/10.1097/01.cji.0000211307.05869.6c

[39] KLAPPE K, HUMMEL I, HOEKSTRA D, KOK JW. Lipid dependence of ABC transporter localization and function. Chem Phys Lipids 2009; 161: 57–64. https://doi.org/10.1016/j.chemphyslip.2009.07.004

[40] FENYVESI F, FENYVESI E, SZENTE L, GODA K, BACSÓ Z et al. P-glycoprotein inhibition by membrane cholesterol modulation. Eur J Pharm Sci 2008; 34: 236–242. https://doi.org/10.1016/j.ejps.2008.04.005

[41] WANG H, JIA XH, CHEN JR, WANG JY, LI YJ. Osthole shows the potential to overcome P-glycoprotein-mediated multidrug resistance in human myelogenous leukemia K562/ADM cells by inhibiting the PI3K/Akt signaling pathway. Oncol Rep 2016; 35: 3659–3668. https://doi.org/10.3892/or.2016.4730

[42] LIU RM, XU P, CHEN Q, FENG SL, XIE Y. A multiple-targets alkaloid nuciferine overcomes paclitaxel-induced drug resistance in vitro and in vivo. Phytomedicine 2020; 79: 153342. https://doi.org/10.1016/j.phymed.2020.153342

[43] ELICH M, SAUER K. Regulation of Hematopoietic Cell Development and Function Through Phosphoinositides. Front Immunol 2018; 9: 931. https://doi.org/10.3389/fimmu.2018.00931

[44] LASSERRE R, GUO X-J, CONCHONAUD F, HAMON Y, HAWCHAR O et al. Raft nanodomains contribute to Akt/PKB plasma membrane recruitment and activation. Nat Chem Biol 2008; 4: 538–547. https://doi.org/10.1038/nchembio.103

https://doi.org/10.4149/neo_2024_240422N179

Disruption of lipid raft reverses drug resistance in colorectal cancer cells through the phosphatase and tensin homolog/phosphoinositide 3-kinase/ protein kinase B pathway and P-glycoprotein

Jing CHEN, Wei ZHENG, Qian LI, RanRan XU, TingTing BAI*, Chao PAN*

Supplementary Information

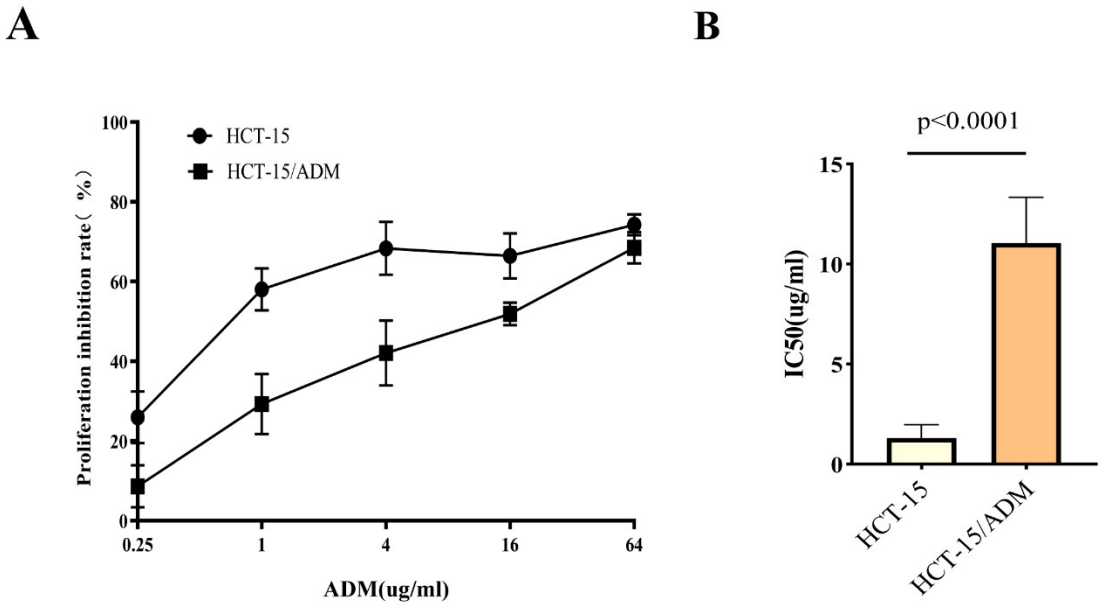

Supplementary Figure S1. HCT-15/ADM showed a significant increase in drug resistance compared with HCT-15. The application of a high dose of ADM (10 μg/ml) induced the recovery of resistance in the resistant cell line (HCT-15/ADM), compared with the parental strain (HCT-15). The resistance index (Half-maximal inhibitory concentration (IC50) of HCT-15/ADM /IC50 of HCT-15) of HCT-15/ADM was 8.4, which indicates moderate resistance and can be used for subsequent experiments.

Supplementary Table S1. Effect of PI3K activator 740Y-P (50 μM) on PIP3/PIP2 values.

Cell line	PIP3/PIP2 ($\times 10^{-3}$)	Upward Fold
HCT-15	2.5±0.1	
HCT-15+740Y-P	2.9±0.3	1.1*
HCT-15/ADM	2.9±0.1	
HCT-15/ADM+740Y-P	3.0±0.4	1.1 (ns)
Con	2.8±0.1	
Con+740Y-P	3.1±0.3	1.1*
Flotillin-1-RNAi	2.6±0.1	
Flotillin-1-RNAi+740Y-P	3.0±0.3	1.2**
Flotillin-2-RNAi	2.6±0.1	
Flotillin-2-RNAi+740Y-P	3.2±0.3	1.2***

*p<0.05; **p<0.01; ***p<0.001

Supplementary Table S2. Effect of PI3K activator 740Y-P (50 μM) on IC50 ADM values.

Cell line	IC50 (ADM μg/ml)	Upward Fold
HCT-15	1.3±0.7	
HCT-15+740Y-P	1.9±1.0	1.4 (ns)
HCT-15/ADM	11.1±2.3	
HCT-15/ADM+740Y-P	14.1±2.5	1.3 (ns)
Con	11.8±1.9	
Con+740Y-P	11.6±1.1	1.0 (ns)
Flotillin-1-RNAi	4.8±1.3	
Flotillin-1-RNAi+740Y-P	7.0±1.5	1.5*
Flotillin-2-RNAi	5.9±1.3	
Flotillin-2-RNAi+740Y-P	18.9±2.8	3.2***

*p<0.05; **p<0.01; ***p<0.001

Supplementary Table S3. Effect of GDC-0941 (4 μM) on PIP3/PIP2 ratio values.

Cell line	PIP3/PIP2 ($\times 10^{-3}$)	Downward Fold
HCT-15	2.5±0.1	
HCT-15+GDC-0941	2.4±0.2	1.0 (ns)
HCT-15/ADM	2.9±0.1	
HCT-15/ADM+GDC-0941	2.5±0.1	1.2*
Con	2.8±0.1	
Con+GDC-0941	2.5±0.1	1.1*
Flotillin-1-RNAi	2.6±0.1	
Flotillin-1-RNAi+GDC-0941	2.3±0.05	1.1*
Flotillin-2-RNAi	2.6±0.1	
Flotillin-2-RNAi+GDC-0941	2.2±0.05	1.1*

*p<0.05; **p<0.01; ***p<0.001

Supplementary Table S4. Effect of GDC-0941 (4 μM) on IC50 ADM values.

Cell line	IC50 (ADM μg/ml)	Reverse Fold
HCT-15	1.3±0.7	
HCT-15+GDC-0941	0.5±0.3	2.6 (ns)
HCT-15/ADM	11.1±2.3	
HCT-15/ADM+GDC-0941	1.4±0.3	7.8***
Con	11.9±1.9	
Con+GDC-0941	1.6±0.3	7.4***
Flotillin-1-RNAi	4.8±1.3	
Flotillin-1-RNAi+GDC-0941	0.3±0.2	16.8***
Flotillin-2-RNAi	5.9±1.3	
Flotillin-2-RNAi+GDC-0941	2.2±1.0	2.7**

*p<0.05; **p<0.01; ***p<0.001

Supplementary Table S5. Effect of P-gp inhibitor Tariquidar (1 μM) on ADM cellular accumulation.

Cell line	ADM level (Fluorescence units)	Increasing Multiple
HCT-15	63.2±8.9	
HCT-15+ Tariquidar	146.0±11.8	2.3***
HCT-15/ADM	6.1±1.7	
HCT-15/ADM+Tariquidar	134.0±9.1	22.0***
Con	4.3±0.8	
Con+ Tariquidar	133.2±6.3	31.0***
Flotillin-1-RNAi	7.3±0.7	
Flotillin-1-RNAi+Tariquidar	144.5±3.8	19.8***
Flotillin-2-RNAi	9.2±1.6	
Flotillin-2-RNAi+Tariquidar	175.7±4.3	19.1***

*p<0.05; **p<0.01; ***p<0.001

Supplementary Table S6. Effect of P-gp inhibitor Tariquidar (1 μM) on IC50 ADM values.

Cell line	IC50 (ADM μg/ml)	Reverse Fold
HCT-15	0.25±0.06	
HCT-15+Tariquidar	0.16±0.06	1.6 (ns)
HCT-15/ADM	7.6±0.1	
HCT-15/ADM+Tariquidar	0.11±0.04	69.1***
Con	9.8±2.1	
Con+ Tariquidar	0.09±0.03	108.9***
Flotillin-1-RNAi	3.1±0.7	
Flotillin-1-RNAi+Tariquidar	0.13±0.02	23.8***
Flotillin-2-RNAi	2.8±1.1	
Flotillin-2-RNAi+Tariquidar	0.22±0.09	12.7***

*p<0.05; **p<0.01; ***p<0.001